Supplementary Information

Rational design of marigold shape composite $Ni_3V_2O_8$ flower: a promising catalyst for oxygen evolution reaction

Rathindranath Biswas[a], Avinava Kundu[a] , Monochura Saha[b], Vishaldeep Kaur[c], Biplab Banerjee[a], Rajendra S. Dhayal[a], Ranjit A. Patil[d], Yuan-Ron Ma[d], Tapasi Sen[c], and Krishna Kanta Haldar[a]*

[a]Department of Chemistry, Central University of Punjab, Bathinda, 151001, India.

[b]Indian Institute of Science Education and Research Kolkata, Nadia 741246, West Bengal, India

[c]Institute of Nano Science and Technology, Mohali, 160062, India.

[d]Department of Physics, National Dong Hwa University, Hualien 97401, Taiwan.

TableS1.ATR-FTIR frequency data (cm^{-1}) of $[Ni(Hq)_2]$ and $[VO(Hq)_2]$ complexes.

Assignments	**$[Ni(Hoq)_2]$ (cm^{-1})**	**$[VO(Hoq)_2]$ (cm^{-1})**	**References**
*v*C=C	1570 1502 1469	1572 1495 1465	1, 2
*v*C-N	1374 1327 1285	1376 1321 1269	2, 3
*v*C-O	1110	1103	4
V=O	-	950	2, 5
out of plan bending of aromatic C-H	820 789 744	835 781 748	4, 6
C-O in plane bending	505	522 500	
Chelate ring deformation	391	402	7, 8
*v*Ni-O	297 278	-	7, 8
*v*Ni-N	258 231	-	7, 8
*v*V-O	-	373 347 301	8, 9
*v*V-N	-	258 233	8, 9

^{1}H NMR and TOF-MS of [Ni(Hq)$_2$] Complex: ^{1}H NMR (DMSO-d_6)δ 15.30 (b, 1H), 17.02 (b, 1H), 18.30 (b, 2H), 20.49 (b, 2H). TOF-MS: m/z $[M+H]^+$calc. for $C_{18}H_{13}N_2O_2Ni$ is 347.0331, found 347.0313 and calc. for $C_{18}H_{12}N_2O_2NiNa$ $[M+Na]^+$ is 360.0150 found 369.0068.

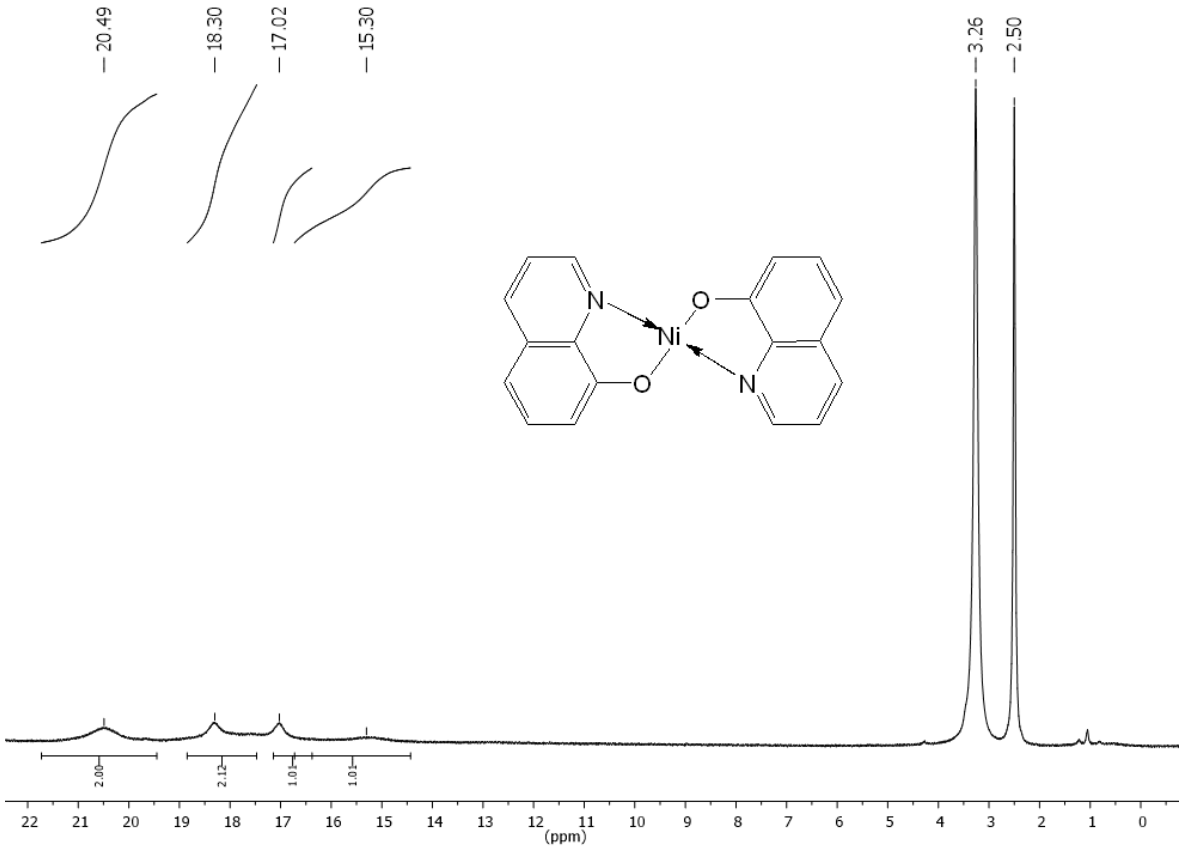

Fig. S1^{1}H NMRspectrum of [Ni(Hq)$_2$] Complex in (DMSO-d_6).

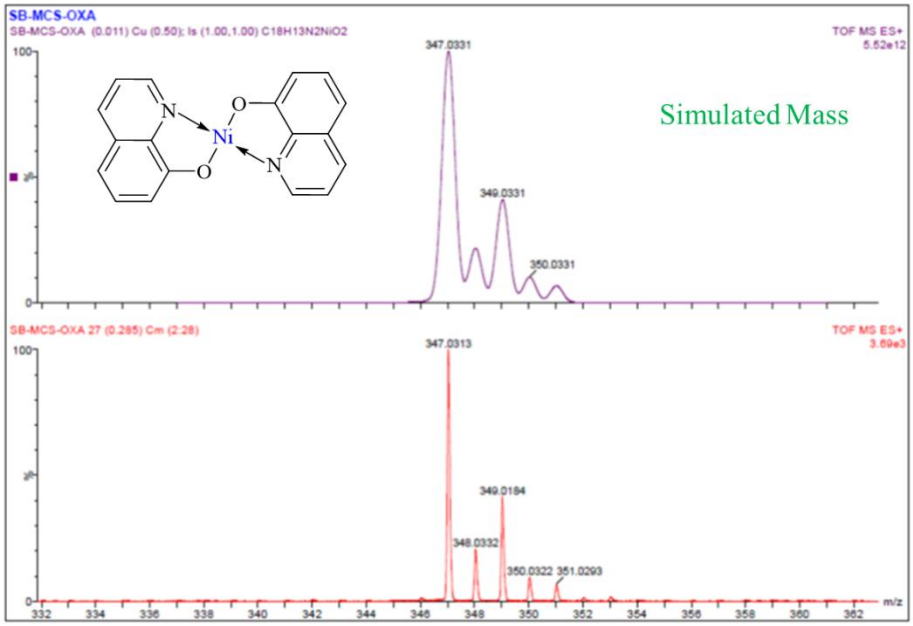

Fig.S2 TOF-MS$[M + H]^+$spectrum of$[Ni(Hq)_2]$ Complex where the magenta line is simulated mass and red line is experimentally found mass.

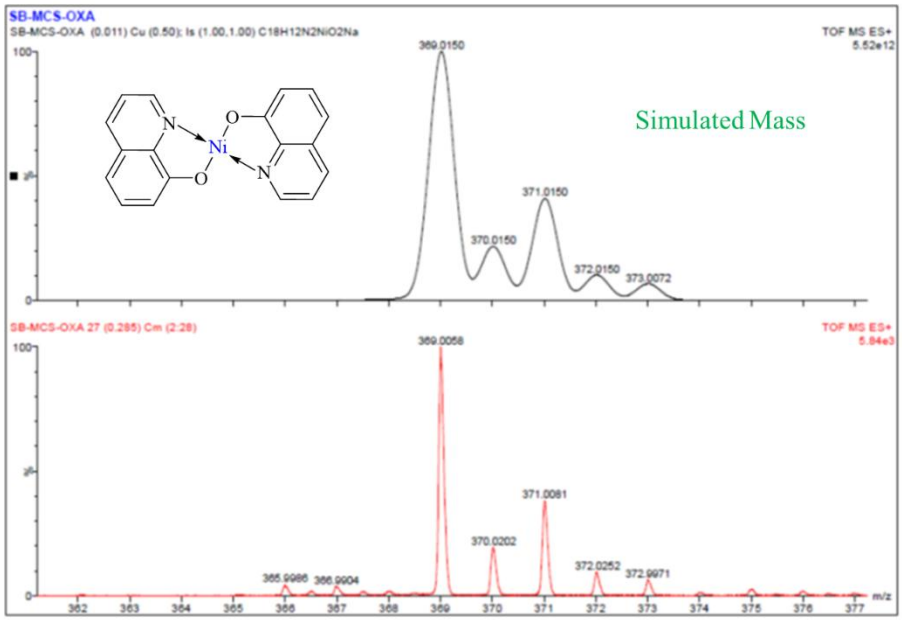

Fig. S3TOF-MS $[M + Na]^+$spectrum of $[Ni(Hq)_2]$ Complex where the black line is simulated mass and red line is experimentally found mass.

^{1}H NMR and TOF-MS of [VO(Hq)$_2$] Complex: ^{1}H NMR (400 MHz, MeOH-d_4) δ 7.14 (d, 2H, 7.96), 7.27 (d, 2H, J = 5.68), 7.58 (mt, 2H), 7.33 (d, 6.4 Hz), 8.17 (d, 1H, J = 4.4 Hz), 8.27 (d, 1H, J = 6.4 Hz), 8.35 (d, 1H, J = 2.92 Hz), 8.56 (d, 1H, *J* = 3.2 Hz). TOFMS: *m/z* $[M+H]^+$calc. for $C_{18}H_{13}N_2O_3V$ is 356.0366, found 356.0314.

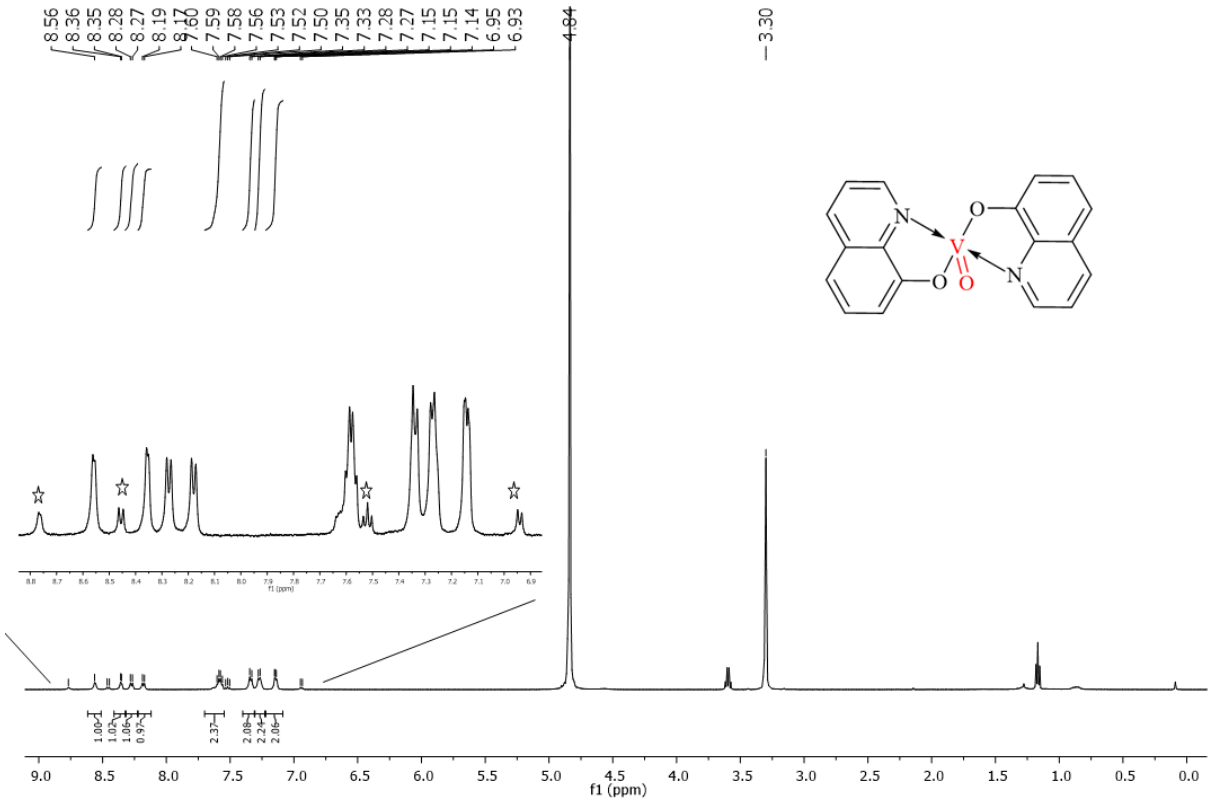

Fig. S4 ^{1}H NMR (MeOH-d_4) spectrum of [VO(Hq)$_2$] Complex (* reveals unreacted Hq).

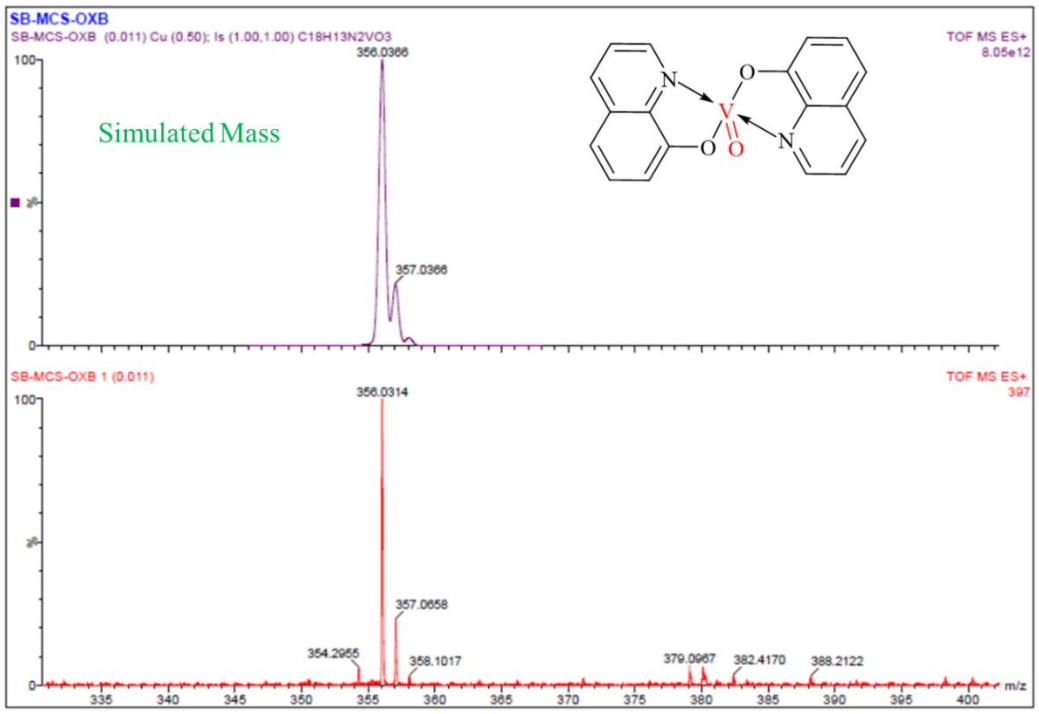

Fig. S5 ESI-MS $[M + H]^+$of $[VO(Hq)_2]$ Complex.

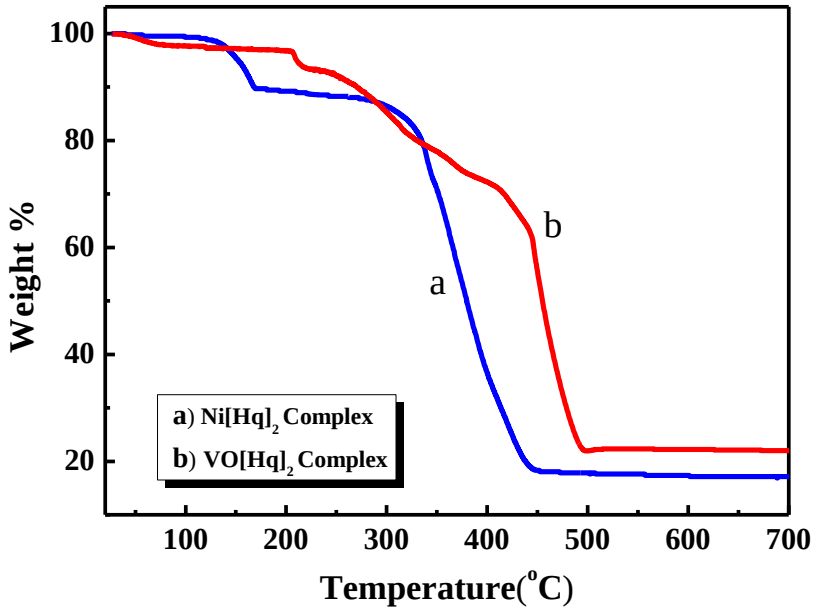

Fig. S6 TGA plot of (a) $[Ni(Hq)_2]$ and (b) $[VO(Hq)_2]$ complexes under nitrogen flow conditions.

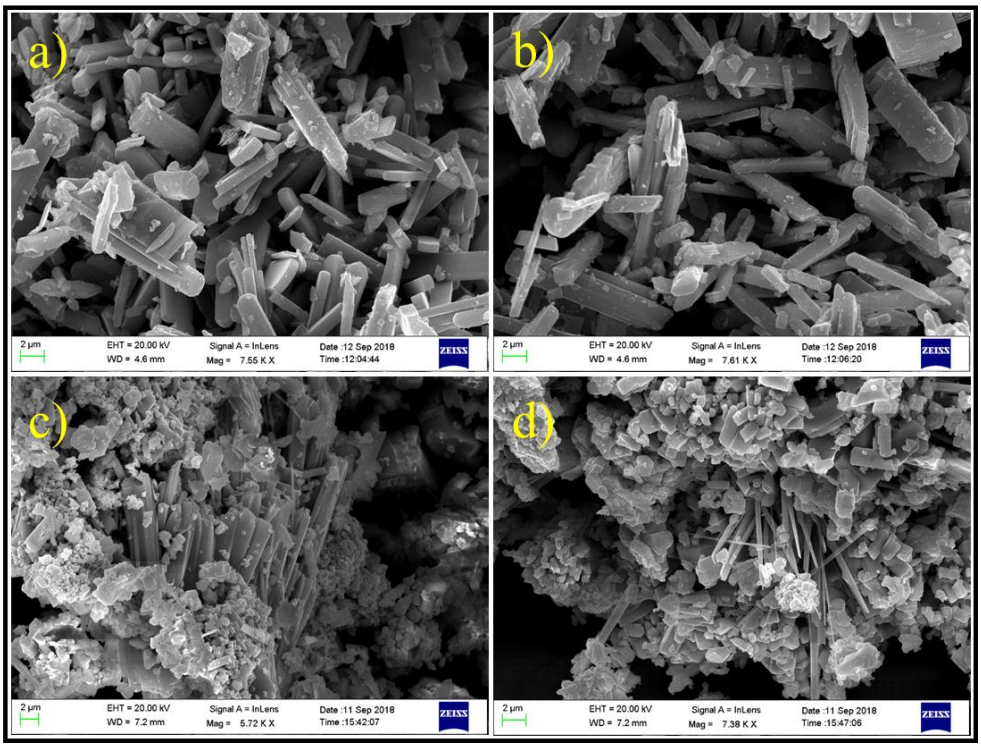

Fig. S7 FE-SEM images of (a-b) NiOand (c-d) V_2O_5 micro rods.

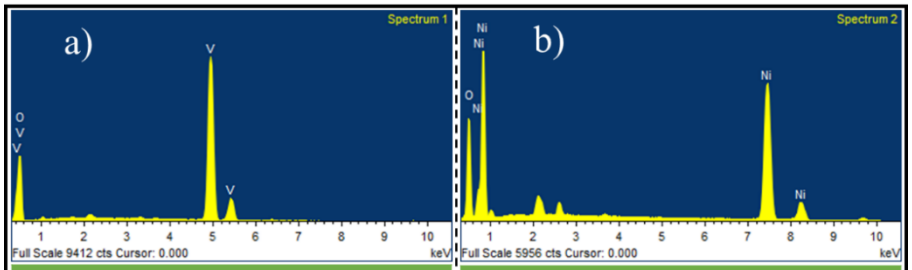

Element	Weight %	Atomic %
O K	40.75	68.66
V K	59.25	31.34
Total	100	100

Element	Weight %	Atomic %
O K	22.90	52.15
Ni K	77.10	47.85
Total	100	100

Fig.S8 Energy dispersive x-ray spectroscopy (EDS) study of (a) V_2O_5 and (b) NiO micro rods.

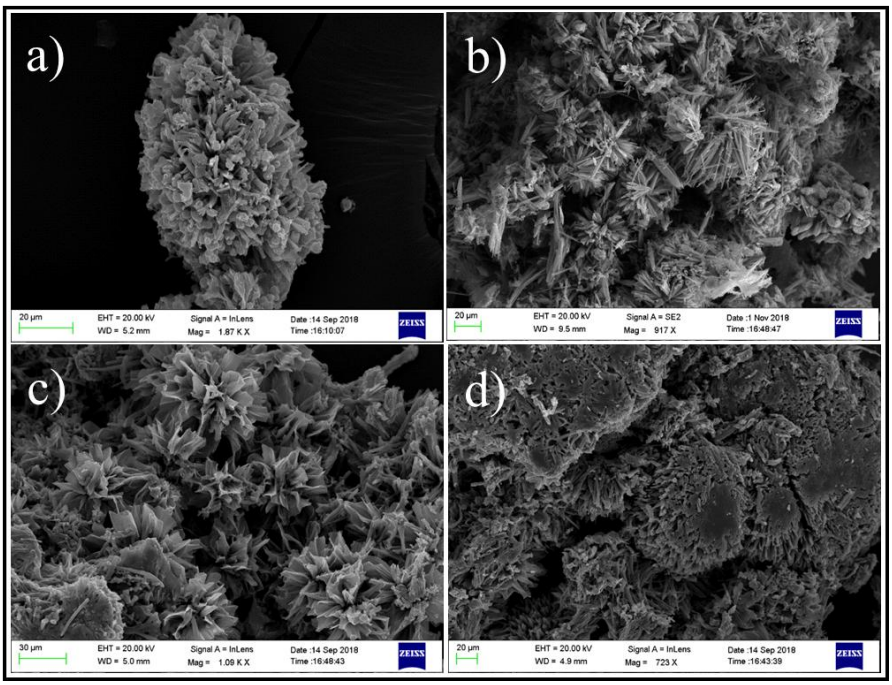

Fig. S9 $Ni_3V_2O_8$ synthesized at different time interval (a) 6h, (b) 16h, (c)24h at 220^oC (d) $Ni_3V_2O_8$ synthesized at at temperature below 190^oC for 72h.

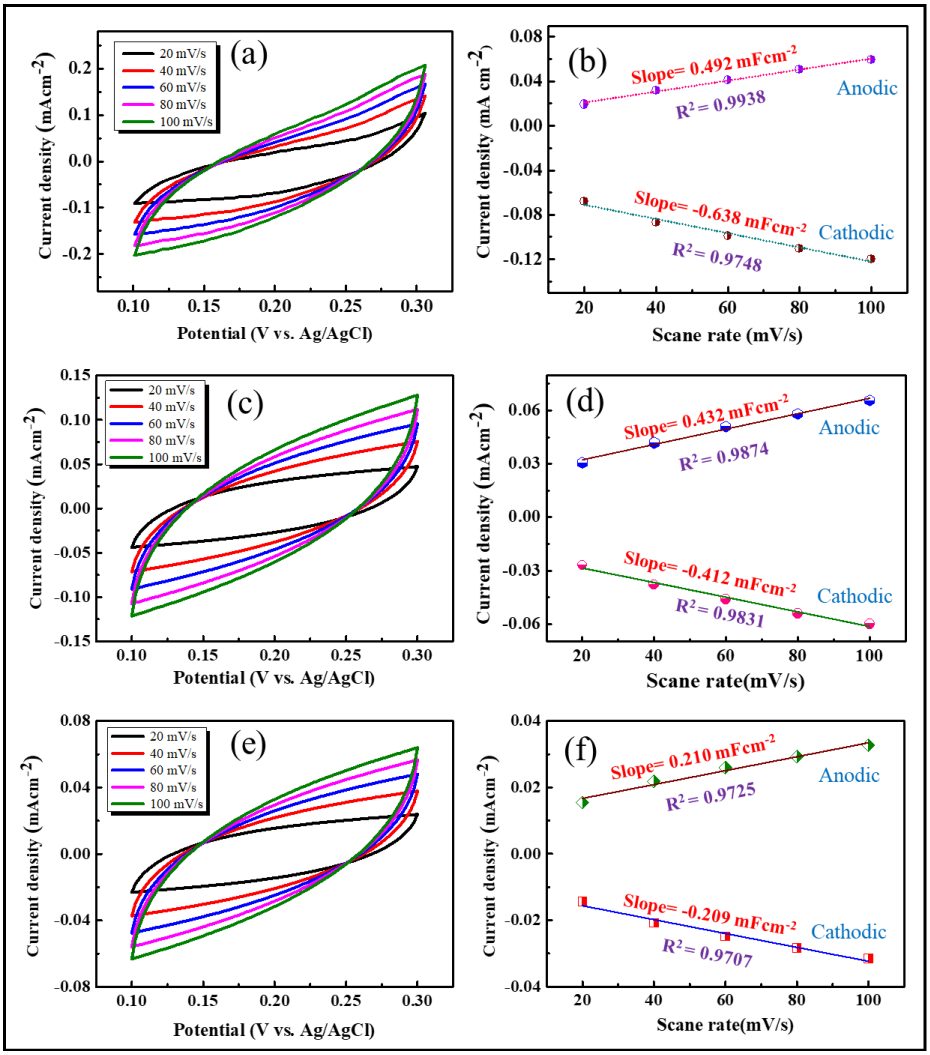

Fig. S10 Cyclic voltammetry curves of (a)physical mixture of V_2O_5 and NiO, (c) NiO, (e)V_2O_5, respectively.Plot of J_a and J_c against scan rate for the determination of double layer capacitance (C_{dl}) for (b) physical mixture of V_2O_5 and NiO, (d) NiO, (f) V_2O_5, respectively.

Electrochemically active surface area: The electrochemically active surface area (ECSA) is proportional to the electrochemical double layer capacitance (C_{dl}) and the value can be calculated using the following equation:

$$ECSA = C_{dl}/C_s$$

Where C_s is the specific capacitance of flat working electrode and its value is 40 μF cm^{-2} per $cm^2{}_{ECSA}$for the flat electrode. The double-layer capacitance (C_{dl}) is calculated from the slope, for

$Ni_3V_2O_8$flower possesses the double-layer capacitance of 2.72 mF cm^{-2}. ECSA is calculated from the obtained C_{dl} by using the above formula and found to be 68 cm^2 for $Ni_3V_2O_8$.

BET analysis:

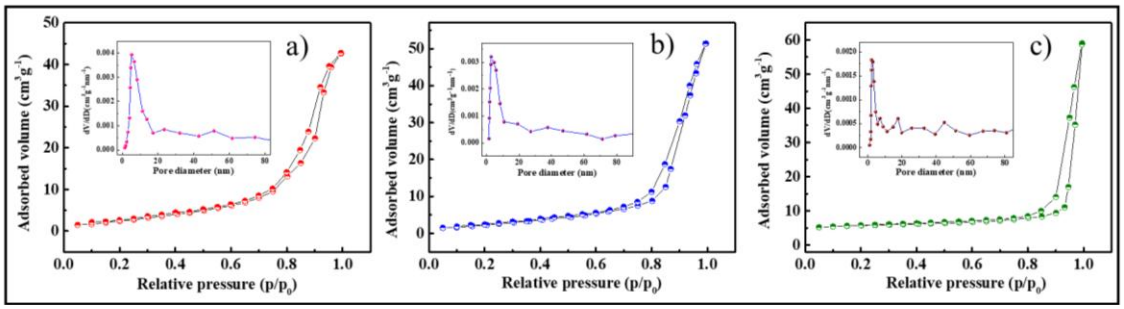

Fig. S11 Nitrogen adsorption–desorption isotherm loop of (a) V_2O_5, (b) NiO and (c) $Ni_3V_2O_8$ flower and insert represents their corresponding the pore size distribution curve calculated by the BJH model.

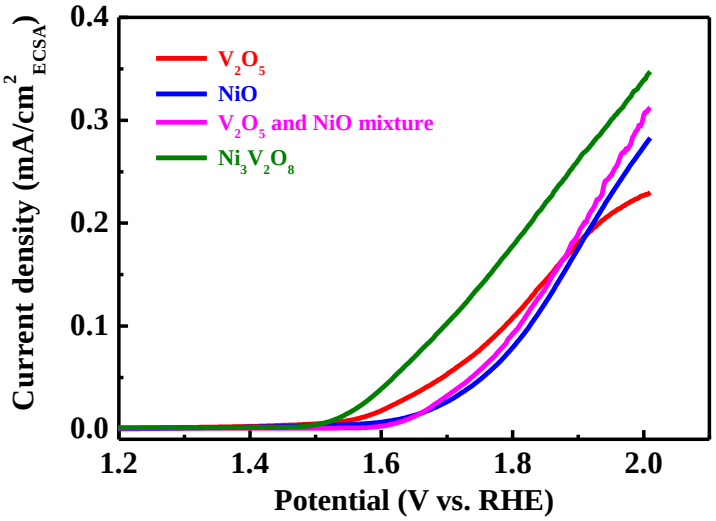

Fig. S12 Polarization curves (normalized by the ECSA) of $Ni_3V_2O_8$, physical mixture of V_2O_5 and NiO, NiO and V_2O_5.

Table S2. A comparison of OER activity of reported binary spinel-structured mixed metal oxide catalyst in literature.

Materials	**Tafel slope (mV dec^{-1})**	**Electrolyte used**	**Massloading (mg cm^{-2})**	**Overpotential**	**References**
Co_3O_4	58.1	1 M NaOH	----	377 mV (10 mA cm^{-2})	10
$CuCo_2O_4$	64	1 M KOH	----	360 mV (10 mA cm^{-2})	11
$CoMn_2O_4$/rGO	56	0.1 M KOH	----	310 mV (10 mA cm^{-2})	12
$NiFeAlO_4$	----	1 M KOH	----	406 mV (10 mA cm^{-2})	13
$NiCo_2O_4$	141	1 M KOH	----	428 mV (10 mA cm^{-2})	14
$NiFe_2O_4$	37	1 M KOH	0.21	262 mV (10 mA cm^{-2})	15
$CoFe_2O_4$	53	0.1 M KOH	0.15	412 mV (5 mA cm^{-2})	16
$ZnCo_2O_4$	46	1 M KOH	----	390 mV (10 mA cm^{-2})	17
$ZnCo_2O_4$	85	0.1 M PBS	----	480 mV (1 mA cm^{-2})	17
$Ni_3V_2O_8$	**61**	**1 M KOH**	**0.19**	**328 mV (10 mA cm^{-2})**	**[This Work]**

References

1. H. Li and Y. Li, *Nanoscale*, 2009, **1**, 128-132.
2. Z. Chi, L. Zhu, X. Lu, H. Yu and B. Liu, *Z. Anorg. Allg. Chem*, 2012, **638**, 1523-1530.
3. R. Biswas, H. Singh, B. Banerjee and K. K. Haldar, *ChemistrySelect*, 2019, **4**, 4003-4007.
4. A. R. Freitas, M. Silva, M. L. Ramos, L. L. Justino, S. M. Fonseca, M. M. Barsan, C. M. Brett, M. R. Silva and H. D. Burrows, *Dalton Trans.*, 2015, **44**, 11491-11503.
5. D. E. Hamilton, *Inorg. Chem.*, 1991, **30**, 1670-1671.
6. N. Karthik, S. Asha and M. Sethuraman, *J. Sol-Gel Sci. Technol.*, 2016, **78**, 248-257.
7. K. Nakamoto and N. Ohkaku, *Inorg. Chem.*, 1971, **10**, 798-805.
8. C. Engelter, G. E. Jackson, C. L. Knight and D. A. Thornton, *J. Mol. Struct.*, 1989, **213**, 133-144.
9. D. A. Thornton, *Vib. Spectrosc.* 1993, **4**, 309-319.
10. H. S. Jeon, M. S. Jee, H. Kim, S. J. Ahn, Y. J. Hwang and B. K. Min, *ACS Appl. Mater. Interfaces*, 2015, **7**, 24550-24555.
11. S. K. Bikkarolla and P. Papakonstantinou, *J. Power Sources*, 2015, **281**, 243-251.
12. J. Du, C. Chen, F. Cheng and J. Chen, *Inorg. Chem.*, 2015, **54**, 5467-5474.
13. J. Y. Chen, J. T. Miller, J. B. Gerken and S. S. Stahl, *Energy Environ. Sci.*, 2014, **7**, 1382-1386.
14. Z. Li, B. Li, J. Chen, Q. Pang and P. Shen, *Int. J. Hydrogen Energy*, 2019, **44**, 16120-16131.
15. H. Yang, Y. Liu, S. Luo, Z. Zhao, X. Wang, Y. Luo, Z. Wang, J. Jin and J. Ma, *ACS Catal.*, 2017, **7**, 5557-5567.
16. C. Si, Y. Zhang, C. Zhang, H. Gao, W. Ma, L. Lv and Z. Zhang, *Electrochim Acta*, 2017, **245**, 829-838.
17. T. W. Kim, M. A. Woo, M. Regis and K.-S. Choi, *J. Phys. Chem. Lett.*, 2014, **5**, 2370-2374.